DOI: 10.1002/adsc.201600629

Advanced Synthesis & Catalysis

*Very Important Publication*

# Radical Stability as a Guideline in C–H Amination Reactions

Davor Šakić[a] and Hendrik Zipse[b,*]

[a] University of Zagreb, Faculty of Pharmacy and Biochemistry, Ante Kovačića 1, 10000 Zagreb, Croatia
[b] Department of Chemistry, LMU Muenchen, Butenandtstrasse 5–13, 81377 Muenchen, Germany
Fax: (+49)-89-2180-77738; phone: (+49)-89-2180-77737; e-mail: zipse@cup.uni-muenchen.de

Received: June 17, 2016; Revised: August 22, 2016; Published online: ■■ ■■, 0000

Supporting information for this article can be found under: http://dx.doi.org/10.1002/adsc.201600629.

**Abstract:** The stability of N-centered radicals and radical cations of potential relevance in C–H amidation reactions has been quantified using highly accurate theoretical methods. Combination with available C–H bond energies for substrate fragments allows for the prediction of reaction enthalpies in 1,5-hydrogen atom transfer (HAT) steps frequently encountered in reactions such as the Hoffman–Löffler–Freytag (HLF) reaction. Protonation of N-radicals is found to be essential in classical HLF reactions for thermochemically feasible HAT steps. The stability of neutral N-radicals depends strongly on the type of *N*-substituent. Among the electron-withdrawing substituents, the trifluoroacetyl (TFA) group is the least and the toluenesulfonyl (tosyl) group the most stabilizing. This implies that TFA-aminyl radicals have the broadest and tosyl-aminyl radicals the smallest window of synthetic applicability. In how far the intramolecular C–H amidation reactions compete with hydrogen abstraction from common organic solvents can be judged based on a comparison of reaction thermodynamics.

**Keywords:** amination; C–H activation; radical stability; remote functionalization

## Introduction

The search for metal-free C–H bond amidation reactions has recently led to a resurgence in studies of what may broadly be seen as variants of the Hoffman–Löffler–Freytag (HLF) reaction.[1–4] Starting from secondary amine substrates these reactions are believed to involve formation of *N*-haloamines as direct precursors of the respective N-centered radicals, generation of which is promoted by photochemical or thermal activation. As illustrated in Scheme 1 for the example of *N*-bromo-2-propylpiperidine (**1**), the strongly acidic reaction conditions used in the classical HLF reaction lead, through thermal or photochemical activation, from bromoaminium ion **2** to transient amine radical cation **3**. Kinetically preferred 1,5-hydrogen atom transfer (1,5-HAT) then leads to formation of C-centered radical **4**, whose halogen atom abstraction from the (protonated) *N*-haloamine substrate **1** closes the radical chain and generates the haloalkylamine product **5**. The final cyclization to 5-membered ring pyrrolidine **6** then follows a classic $S_N2$ mechanism and often requires basic reaction conditions. That a similar sequence can be developed under neutral conditions has been demonstrated by Corey et al. for the example shown in Scheme 2.[5a] Building on earlier work by Barton et al. on lactone syntheses,[5b] trifluoroacetamide **7** is in this case first transformed quantitatively to bromoamide **8**.

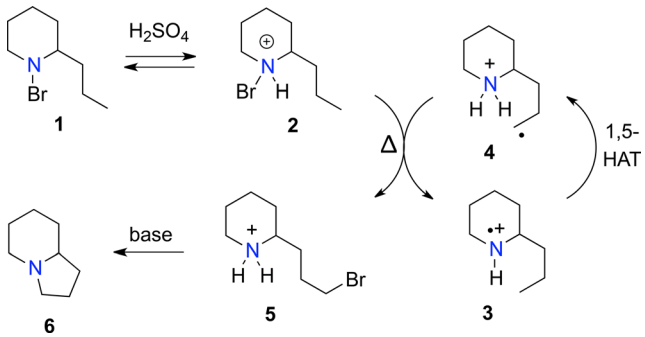


**Scheme 1.** Essential mechanistic steps in the classical HLF reaction of bromopiperidine **1** under acidic conditions.

Photochemical activation of this precursor is in this case believed to generate amidyl radical **9**, followed by a 1,5-HAT step to generate substrate radical **10**. The radical chain is again completed by bromine abstraction from (neutral) precursor **8** to yield bromide **11**. Base-induced cyclization then yields the final proline derivative **12**. More recently variants of the HLF reaction integrate precursor synthesis, (photochemi-

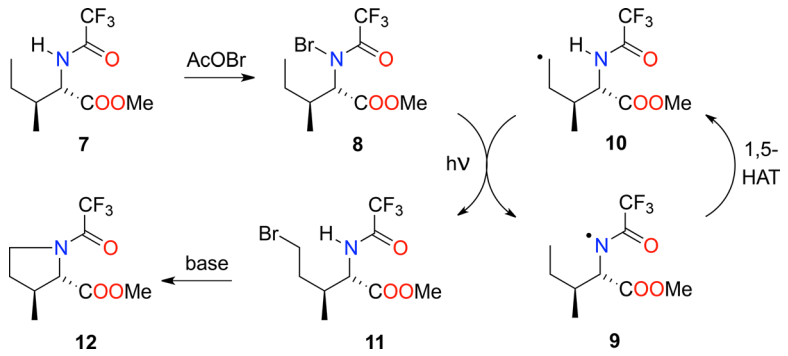


**Scheme 2.** Essential mechanistic steps in the "Corey modification" using *N*-bromoisoleucine derivative **8** as an example.

cal) C–H bond activation and cyclization reaction into one synthetic step. In many of these cases loosely referred to as "Suarez modification"[6–10] hypervalent iodine reagents such as diacetoxyiodobenzene (DAIB) are used as oxidants, often in combination with $I_2$ as the co-catalyst/co-oxidant.[3,11,12] Efforts to optimize the synthetic utility of this modification have shown that the reaction outcome depends critically on the actual nature of the oxidant(s), the reaction conditions (choice of solvent, reaction temperature, mode of initiation) and the substrate substitution pattern.[1,13–18]

A typical example involves tosylamide **13**, whose photochemically driven reaction with $I_2$/DAIB yields pyrrolidine **18** in 67% yield.[13] As in the other variants shown in Scheme 1 and Scheme 2 these transformations are believed to involve the initial formation of *N*-halo derivatives such **14**, their photochemical activation to N-centered radicals **15**, C–H bond activation through 1,5-hydrogen atom transfer, and final trapping of the substrate radical through halogen transfer (Scheme 3). Cyclization of iodide **17** to product **18** may then follow a base-induced or alternative pathway. All three HLF variants shown in Scheme 1, Scheme 2, and Scheme 3 involve C–H bond activation through neutral or cationic aminyl radicals, and the success of the overall HLF scheme thus depends on the efficiency of this reaction step. While C–H bond energies are well known and documented in the literature for a wide variety of hydrocarbons, this is not so for N–H bond energies in amines, amides, and their protonated counterparts. The thermodynamic driving force behind the 1,5-HAT steps shown in Scheme 1 can therefore not be estimated using existing bond dissociation energy (BDE) data. In an effort to provide an appropriate dataset for the design and implementation of novel HLF reaction schemes, we have now calculated the required N–H bond dissociation energies and associated stability values of N-centered radicals.

## Results

The stabilities of aminyl radicals relative to the unsubstituted aminyl radical $^{\cdot}NH_2$ (**19**) have been calculated as the reaction enthalpies at 298.15 K for the hydrogen transfer reaction shown in Eq. (1). In the following these will be referred to as radical stabilization energies (RSEs) of the respective N-centered radical **R**. Addition of the RSE values calculated according to Eq. (1) to the experimentally known N–H bond dissociation energy in ammonia of $BDE(H_2N–H) = +450.1 \pm 0.24$ kJ/mol[19] yields the N–H bond dissociation energy (BDE) values in the respective amine and amide parent compounds.

Thermochemical calculations have been performed using the same hierarchy of theoretical methods as

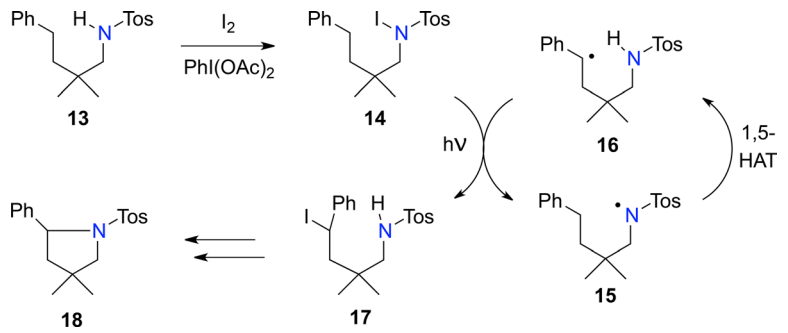


**Scheme 3.** Essential mechanistic steps in the "Suarez modification" using sulfonamide **13** as an example.

 

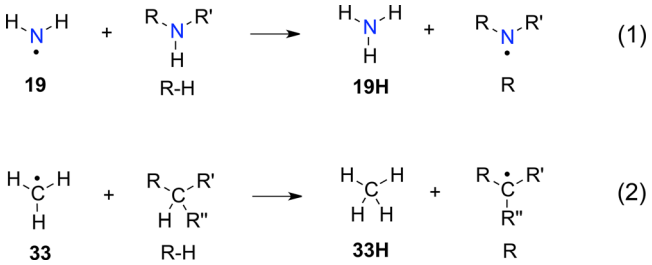


before ranging from (U)B3LYP/6-31G(d)[20,21] as an entry-level hybrid DFT method, the double hybrid ROB2-PLYP[22] method, and the highly accurate G3(MP2)-RAD[23] and G3B3[24] compound schemes. Only the latter (most accurate) results will be discussed in the following, if not noted otherwise.

The least stable N-centered radicals studied here are aminyl radicals combining a trifluoroacetyl and an alkyl substituent. The stability values show little dependence on the choice of alkyl group and range from with RSE(**20.1**) = +18.8 kJ/mol for R = isopropyl to RSE(**20.6**) = +14.6 kJ/mol for R = *n*-butyl (Figure 1, Table 1). Replacement of the TFA group by the acetyl (as in **22**) or the Boc group (as in **21**)

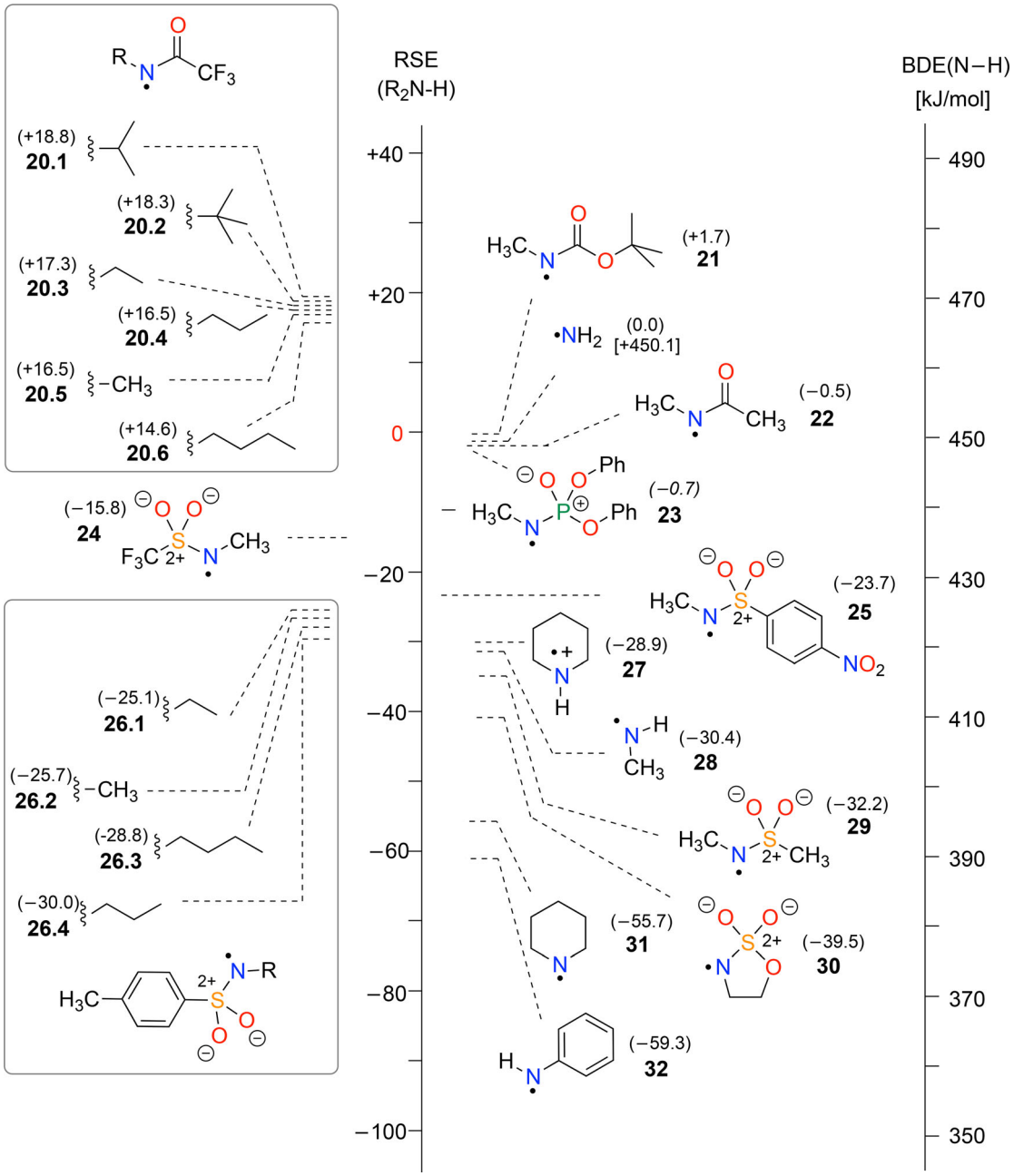


**Figure 1.** Radical stabilization energies (RSEs) and bond dissociation energies (BDEs) for selected N-centered radicals (in kJ/mol).

 

**Table 1.** Gas phase radical stabilization energies (RSE) calculated according to Eq. (1) for the N-centered radicals shown in Figure 1 together with the BDE(N–H) values in the corresponding closed-shell parent systems (in kJ/mol).[a]

| R | RSE (ROB2-PLYP)[b] | RSE (G3(MP2)-RAD) | RSE (G3B3) | BDE (calcd.) | BDE[c] (exp.) |
|---|---|---|---|---|---|
| **20.1** | +18.6 | +19.8 | +18.8 | +468.9 | |
| **20.2** | +16.5 | +20.8 | +18.3 | +468.4 | |
| **20.3** | +16.1 | +18.1 | +17.3 | +467.4 | |
| **20.4** | +14.2 | +17.6 | +16.5 | +466.6 | |
| **20.5** | +15.9 | +16.8 | +16.5 | +466.6 | |
| **20.6** | +14.5 | +15.6 | +14.6 | +464.7 | |
| **21** | −1.1 | +2.2 | +1.7 | +451.8 | |
| **19** | 0.0 | 0.0 | 0.0 | +450.1 | +450.1 ± 0.2 |
| **22** | +0.4 | +2.1 | −0.5 | +449.6 | +445.6 ± 12.6 |
| **23** | −8.8 | −0.7 | – | +449.4 | |
| **24** | −20.9 | −15.2 | −15.8 | +434.3 | |
| **25** | −29.4 | −23.1 | −23.7 | +426.4 | |
| **26.1** | −32.7 | −28.6 | −25.1 | +425.0 | |
| **26.2** | −31.8 | −22.8 | −25.7 | +424.4 | |
| **26.3** | −36.4 | −28.8 | – | +421.3 | |
| **27** | −40.0 | −28.0 | −28.9 | +421.2 | |
| **26.4** | −35.5 | −28.6 | −30.0 | +420.1 | |
| **28** | −33.9 | −30.0 | −30.4 | +419.7 | +425.1 ± 8.4 |
| **29** | −36.7 | −31.0 | −32.2 | +417.9 | |
| **30** | −43.5 | −37.8 | −39.5 | +410.6 | |
| **31** | −52.4 | −49.7 | −55.7 | +402.8 | |
| **32** | −61.0 | −65.7 | −59.3 | +390.8 | |

[a] Ordered by RSE values calculated at G3B3 level. For radicals **23** and **26.3** G3(MP2)-RAD results have been used instead.
[b] ROB2-PLYP/G3MP2large//UB3LYP/6-31G(d) results.
[c] Taken from ref.[19]

yields significantly more stable amidyl radicals with stability values around zero. From the sulfonylamidyl radicals considered here the least stable is trifluoromethylsulfonylamidyl radical **24** with RSE(**24**) = −15.8 kJ/mol. The least stable phenylsulfonylamidyl radical is **25** with RSE(**25**) = −23.7 kJ/mol. Replacing the *para*-substituent in **25** by a methyl group as in radical **26.2** causes only a minor change towards higher RSE values with RSE(**26.2**) = −25.7 kJ/mol. Changing from the trifluoromethyl substituent in **24** to a methyl substituent in radical **29** leads to a significantly more stable radical with RSE(**29**) = −32.2 kJ/mol. The most stable sulfonylamidyl radical considered here is **30** with RSE(**30**) = −39.5 kJ/mol. How N-radical stability responds to variations in the alkyl group attached to the N-atom was explored for sulfonamide radical **26.2** as the most typical representative of its class. As found before for the trifluoracetylaminyl radicals, the stability of sulfonamidyl radicals shows little dependence on the choice of the alkyl groups and ranges from RSE(**26.1**) = −25.1 kJ/mol for R = ethyl to $RSE_{G3(MP2)\text{-}RAD}$(**26.4**) = −30.0 kJ/mol$^{-1}$ for R = *n*-propyl. Finally, the diphenylphosphoryl-substituted aminyl radical **23** is slightly more stable than the parent aminyl radical **19**, but clearly less stable than all sulfonylamidyl radicals. The acceptor-substituted aminyl radicals discussed above are all less stable than typical secondary aminyl radicals such as piperidinyl radical **31** with RSE(**31**) = −55.7 kJ/mol.[25] This value is reduced through protonation by 26.8 kJ/mol, which implies RSE(**27**) = −28.9 kJ/mol for piperidinium radical cation **27**.

Experimental data for N–H bond energies/RSE values appear to exist for only two of the N-centered radicals shown in Figure 1. RSE(**22**) = −4.5 ± 12.6 kJ/mol and RSE($CH_3(H)N^{\cdot}$, **28**) = −25.8 ± 8.4 kJ/mol.[19] The G3B3 values shown in Figure 1 for these two species fall into the experimental error range. This suggests that the remaining RSE values are unlikely to be grossly wrong.

Reaction energies for HAT reactions from hydrocarbon substrates depend on the stability of the reacting aminyl radicals as well as the stability of the newly generated C-radicals. Stability values for selected C-centered radicals calculated according to Eq. (2) have therefore been collected in Table 2 and are shown in Figure 2 in a pictorial manner. These RSE values can be converted to C–H bond dissociation energies in the respective hydrocarbon precursors through addition to the experimentally determined BDE(C–H) value of methane (**33H**) of BDE(C–H, **33H**) = +439.3 ± 0.4 kJ/mol.[19] The C-centered radi-

**Table 2.** Radical stabilization energies (RSE) calculated according to Eq. (2) for the C-centered radicals shown in Figure 2 together with BDE(C–H) values in the respective closed-shell parent systems (in kJ/mol).[a]

| R | RSE (ROB2-PLYP)[b] | RSE (G3(MP2)-RAD) | RSE (G3B3) | BDE (calcd.) | BDE (exp.)[c] |
|---|---|---|---|---|---|
| **34** | | +36.9[d] | +42.0[d] | +473.4 | +472.2 ± 2.2 |
| **33** | 0.0 | 0.0 | 0.0 | +439.3 | +439.3 ± 0.4 |
| **35** | −15.5 | −12.2 | −12.5 | +426.8 | +422.2 ± 2.1 |
| **36** | | −13.5[e] | −13.8[e] | +424.2 | +420.5 ± 1.3 |
| **37** | | −23.0[e] | −23.7[e] | +415.6 | +410.5 ± 2.9 |
| **38** | −33.7 | −26.0 | −27.3 | +412.0 | – |
| **39** | −36.5 | −32.5[e] | −33.6 | +405.6 | +405.8 ± 4.2 |
| **40** | −38.6 | −32.2[e] | −34.2 | +405.1 | +407.1 ± 4.2 |
| **42** | −48.9 | −43.4 | −44.1 | +395.2 | – |
| **41** | −51.6 | −42.5[e] | −44.4 | +397.0 | +392.5 ± 2.5 |
| **43** | −50.9 | −43.5 | −44.9 | +394.4 | +385.3 ± 6.7 |
| **44** | | −61.0[e] | −55.1[e] [−61.2][e,f] | +384.2 [+378.1] | +375.7 ± 2.5[g] |
| **45** | −71.3 | −68.3[e] | −62.7 | +376.6 | |

[a] Ordered by RSE values calculated at G3B3 level.
[b] ROB2-PLYP/G3MP2large//UB3LYP/6-31G(d) results.
[c] Taken from ref.[19]
[d] Taken from ref.[26]
[e] Taken from ref.[27]
[f] W1 result.
[g] Taken from ref.[28]

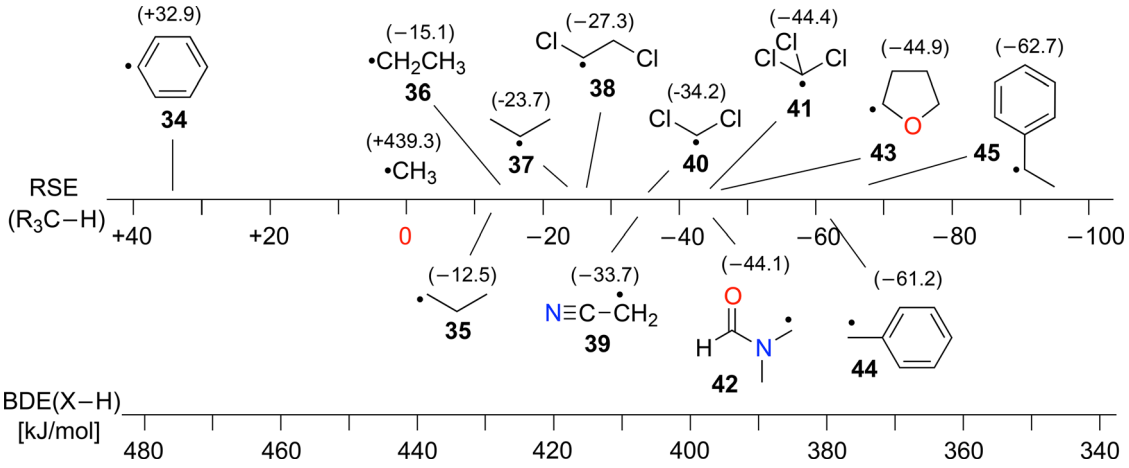


**Figure 2.** Radical stabilization energies (RSEs) and bond dissociation energies (BDEs) for selected C-centered radicals (in kJ/mol).

cals selected here are either those derived from frequently used organic solvents or those representative for structural fragments in hydrocarbon substrates.

Benzene (**34H**) and toluene (**44H**) are among the most often used solvents for radical reactions. However, in terms of C–H bond energies these two solvents differ largely in that hydrogen abstraction from benzene is endothermic for all N-centered radicals collected in Table 1, while the corresponding reactions with toluene are all exothermic. The stability of radicals derived from chlorinated solvents such as dichloromethane (**40H**) or chloroform (**41H**) is smaller than that of the toluene-derived benzyl radical. The C-centered radical **38** obtained through hydrogen abstraction from 1,2-dichloroethane (DCE, **38H**) is even less stable than **40** or **41** with RSE(**38**) = −27.3 kJ/mol, while the opposite is observed for radicals obtained from the more polar solvents acetonitrile (**39H**), *N*,*N*-dimethylformamide (DMF, **42H**), or tetrahydrofuran (THF, **43H**).

Assuming that *n*-propyl radical **35** with RSE(**35**) = −12.5 kJ/mol and isopropyl radical **37** with RSE(**37**) = −23.7 kJ/mol are suitable prototypes for primary and secondary substrate radicals generated through intramolecular hydrogen abstraction, it is remarkable to see that all solvent-derived radicals (except phenyl

radical **34**) collected in Table 2 and shown in Figure 2 are more stable than these substrate radicals. This implies that any advantage towards intramolecular hydrogen abstraction from unactivated hydrocarbon side chains as compared to hydrogen abstraction from the solvent is entirely due to kinetic factors! The situation changes completely on introduction of radical-stabilizing substituents next to the prospective substrate radical center, and benzylic radical **45** with RSE(**45**) = −62.7 kJ/mol$^{-1}$ may be typical for this situation.

## Discussion

In topological terms all hydrogen atom transfer steps shown in the three C–H amidation reactions in Scheme 1, Scheme 2, and Scheme 3 are of the "1,5-HAT" type. Despite this apparent similarity, the thermochemical profiles of these transformations are dramatically different. This can be seen by putting together the overall reaction enthalpies from the BDE(C–H) and BDE(N–H) values for typical fragments contained in the respective reactants and products. For the classical HLF reaction starting from bromoamide **1**, the key 1,5-HAT step converts N-radical cation **3** to C-radical **4**. The BDE(C–H) value for the reacting C–H bond can in this case be assumed to be close to that in the terminal position of propane. As indicated with the grey shaded fragment in Scheme 4a, this implies a BDE(C–H) value of +426.8 kJ/mol. The N–H bond formed in the 1,5-HAT step can be assumed to be closely similar to that in the piperidinium cation. The BDE(N–H) value in this latter fragment shown in grey in Scheme 4a amounts to +421.2 kJ/mol. Taken together this implies a 1,5-HAT reaction enthalpy of $\Delta H_{298}$(**4a**) = 426.8–421.2 = +5.6 kJ/mol. Comparison of this slightly endothermic step with that in the respective neutral system (Scheme 4b) shows how important the highly acidic reaction medium is for the HLF reaction: due to the much weaker N–H bond in neutral piperidine as compared to the piperidinium cation the driving force for the 1,5-HAT step is much more positive at $\Delta H_{298}$(**4b**) = +24.0 kJ/mol$^{-1}$ for the neutral system. Protonation of the bromoamide precursor in HLF reactions is thus not only relevant from a kinetic point of view, but also for a thermochemically feasible HAT step!

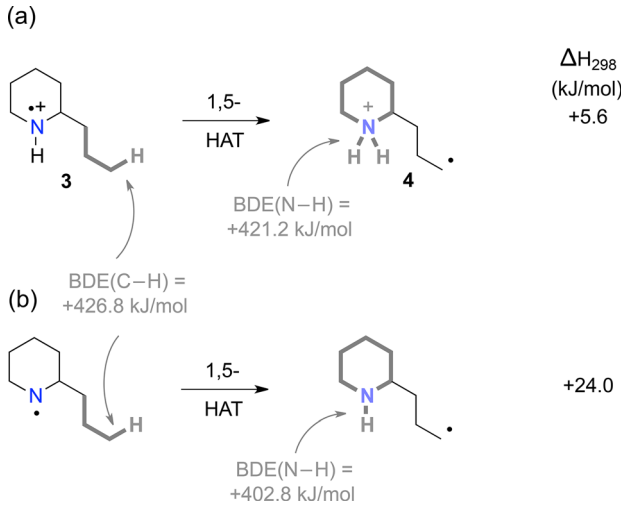


**Scheme 4.** Thermochemical profiles for 1,5-HAT steps in the HLF reaction of bromoamine **1** (a) for protonated; and (b) for non-protonated substrate radicals.

In order to evaluate the accuracy of the fragment-based approach, G3B3 calculations have been performed for the full substrates shown in Scheme 4a (cationic) and Scheme 4b (neutral). A reaction enthalpy of $\Delta H_{298}$(**4b**) = +28.8 kJ/mol is calculated for the neutral system shown in Scheme 4b, which is 4.8 kJ/mol more endergonic as compared to the fragment-based approach. For the radical cation variant of this transformation shown in Scheme 4a, the reaction enthalpy is slightly exothermic at $\Delta H_{298}$(**4a**) = −1.9 kJ/mol, a reduction of 7.5 kJ/mol as compared to the fragment-based approach.

Reaction of the cationic substrate shown in Scheme 4a may be more influenced by solvent effects than reactions of neutral radicals. The gas phase results presented above were therefore combined with aqueous solvation free energies calculated with the SMD continuum solvation model[29] and the (U)B3LYP/6-31G(d) hybrid functional. Due to better solvation of reactant radical **3** as compared to product radical **4** by $\Delta\Delta G_{solv}$ = +5.0 kJ/mol, the overall reaction becomes moderately endothermic in water with $\Delta H_{298}$(**4a**) = +3.1 kJ/mol. We may thus conclude that, even for transformations involving radical cations, the fragment-based approach using gas phase BDE values yields reaction enthalpies quite close to those using full substrate models in solution, most likely due to the cancellation of various errors.

Following essentially the same logic as for the classical HLF reaction of substrate **1**, the thermochemical profile for the 1,5-HAT step in the "Corey modification" with substrate **7** can be analyzed. Using again the BDE values calculated for the grey shaded fragments shown in Scheme 5a at G3B3 level, the 1,5-HAT reaction transforming N-centered radical **9** to C-centered product radical **10** is exothermic by $\Delta H_{298}$(**5a**) = −39.8 kJ/mol.[30]

Calculations on the full systems **9**/**10** predict an even larger exothermicity of $\Delta H_{298}$(**5a**) = −45.8 kJ/mol, reflecting the electron-withdrawing effect of the methoxycarbonyl substituent adjacent to the N-radical site.[31] The trifluoroacetyl substituent is thus quite effective in destabilizing the N-centered radical sufficiently well for an overall exothermic HAT step.

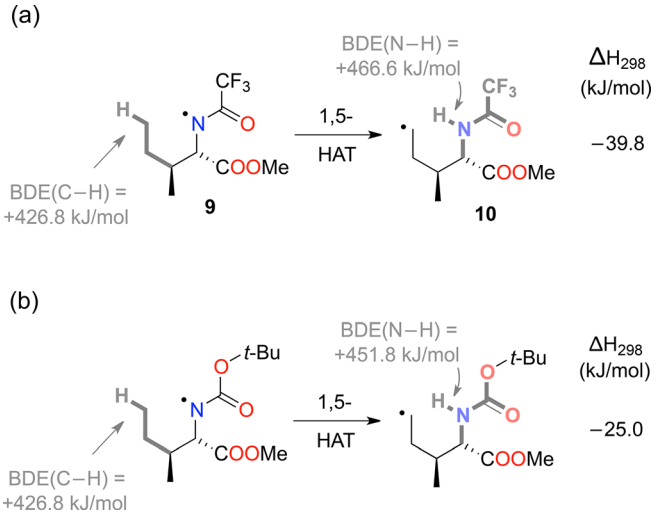


**Scheme 5.** Thermochemical profile for 1,5-HAT steps in the "Corey modified" HLF reaction involving amide **7** and a Boc-protected substrate analogue.

Other acyl groups are less effective in this respect as can be seen from the less positive RSE values for acetyl- and Boc-substituted aminyl radicals in Figure 1.

Replacing the trifluoroacetyl by the Boc-protecting group in radical **9**, for example, reduces the 1,5-HAT reaction enthalpy to $\Delta H_{298}$(**7b**) = −25.0 kJ/mol (Scheme 5b). Exploring this latter example in practice, Corey et al. indeed noted significantly lower yields of product as compared to the trifluoroacetyl system.[5] Despite the fact that reaction yields and 1,5-HAT reaction enthalpy show a common trend in this case, the actual reaction outcome will also be influenced by other factors such as the conformational preferences of substituents of different size as well as polar effects in the 1,5-HAT transition states.

Continuing this type of analysis for the HLF "Suarez modification" for the example of sulfonamide **13**, we note that the sulfonamide radical **15** involved in this transformation is significantly more stable than the amide radicals discussed in Scheme 5. Sulfonamide radical **26.3** with RSE(**26.3**) = −28.8 kJ/mol may be considered to be the most appropriate model here as indicted by the grey shaded substructure. That the 1,5-HAT step leading to substrate radical **16** is exothermic with $\Delta H_{298}$(**6a**) = −44.7 kJ/mol is thus mainly due to the stability of the benzylic radical formed (Scheme 6)! Modification of the system such that a less stable secondary aliphatic product radical is generated as in the 1,5-HAT step interconverting radicals **46** and **47**, the driving force is significantly reduced to only $\Delta H_{298}$(**6b**) = −5.7 kJ/mol. This fragment-based estimate is remarkably close to the value $\Delta H_{298}$(**6b**) = −5.9 kJ/mol obtained at G3(MP2)-RAD level for the complete systems **46**/**47**. That *intramolecular* HAT reactions with such small endothermicities

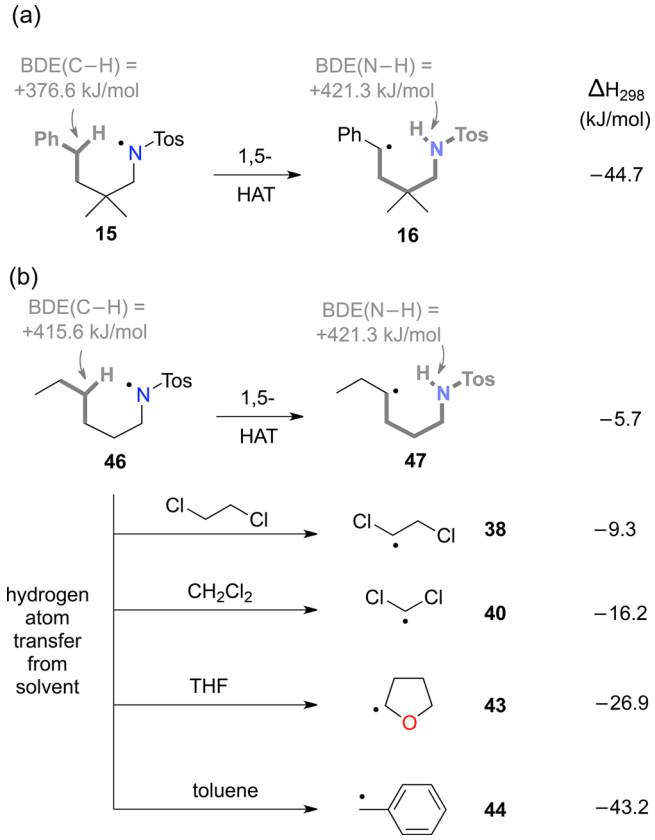


**Scheme 6.** Thermochemical profiles for hydrogen atom transfer (HAT) steps involving sulfonamide radicals.

may have to compete with *intermolecular* HAT reactions with solvent molecules is easily demonstrated by calculating the respective reaction enthalpies. Already for 1,2-dichloroethane (DCE) as an often used solvent for the $I_2$/DAIB combination the intermolecular HAT reaction is more exothermic at $\Delta H_{298}$(**6b**/**38**) = −9.3 kJ/mol. For dichloromethane (DCM) a closely similar exothermicity of $\Delta H_{298}$(**6b**/**40**) = −16.2 kJ/mol is obtained, while the reactions become much more exothermic for solvents with weaker C–H bonds such as for THF [$\Delta H_{298}$(**6b**/**43**) = −26.9 kJ/mol] or for toluene [$\Delta H_{298}$(**6b**/**44**) = −43.2 kJ/mol].

The competition between intra- and intermolecular HAT steps may, at least in part, be responsible for significant solvent effects observed for reactions involving sulfonamide radicals.[14,15,32] One example concerns the cyclization of *N*-hexylsulfonamide **48** to 2-ethylpyrrolidine derivative **49** (Scheme 7). This cyclization, which is believed to involve formation of sulfonamide radical **46** and its transformation to radical **47** through the 1,5-HAT step shown in Scheme 6, proceeds with good yield in 1,2-dichloroethane as the solvent at room temperature. Somewhat lower yields are obtained in dichloromethane, while the reaction ceases to work in THF or toluene. The outcome of this cyclization thus parallels the exothermicity of the

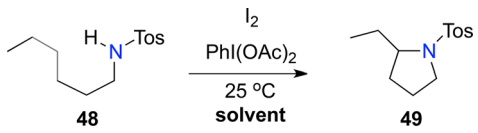


| solvent | yield [%] |
|---|---|
| Cl, Cl | 82 |
| $CH_2Cl_2$ | 42 |
| THF | – |
| toluene | – |

**Scheme 7.** Cyclization of sulfonamide **48** under Suarez conditions as reported by Fan et al.[16].

solvent HAT reactions described in Scheme 6. The weak α-C–H bond in THF (and the stability of the respective THF radical **43**) has actually inspired recent successful efforts to turn this unwanted side reaction into the main substrate reaction.[33]

It should be added that not all solvent effects are due to competing HAT reactions, and particularly polar and/or protic solvents may interfere with generation of the N-halo precursor more than with the actual radical chemistry.

## Conclusions

We have demonstrated the utility of quantifying the thermochemistry of intra- and intermolecular HAT reactions involving neutral and cationic N-centered radicals. With the new results for the stability of N-centered radicals in hand the design of transformations involving new substrate scaffolds can be based on C–H bond energies available in the literature for a variety of representative fragments.[1] This type of analysis will be particularly helpful in order to avoid reactions involving endothermic HAT steps. The overall efficiency of HLF reaction schemes depends, of course, on a number of additional factors such as the efficiency of N-radical generation as well as polar and steric effects in the HAT transition states. The limits for this type of thermochemical analysis are also reached where the reaction mechanism involves transient cationic (instead of radical) intermediates.[34]

## Experimental Section

### Theoretical Methods

Initial structures for geometry optimizations have been generated for the closed shell systems using a systematic stepwise rotation (30°) around variable dihedral angles. After elimination of structures showing non-bonded interatomic distances of less than 100 pm, geometry optimization was performed for all structures at the B3LYP/6-31G(d)[20,21] level of theory. Geometry optimizations for open shell species were performed at the UB3LYP/6-31G(d)[20,21] level of theory starting from all conformational minima found for the respective closed shell parent systems after removal of selected hydrogen atoms. Different electronic states of the open shell species were analyzed using the suitable manipulation of the initial guess alpha/beta orbitals. Standard convergence criteria and the default "finegrid" integration grid size have been used in all cases. Thermal corrections to enthalpies at 298.15 K have been calculated using the rigid rotor/harmonic oscillator model and a scaling factor of 0.9806 as employed in the G3(MP2)-RAD compound scheme.[23] Subsequent single point calculations have been performed at the ROB2-PLYP/G3MP2large level.[22] Combination of the ROB2-PLYP energies with thermochemical corrections to 298.15 K obtained at (U)B3LYP level yield the energies employed to calculate the "RSE(ROB2-PLYP)" values in Table 1 and Table 2. Refined BDE(N–H) and RSE values have then been calculated using the G3(MP2)-RAD[23] and G3B3[24] compound schemes. Solvation free energies were calculated for water using single point calculations with the SMD continuum solvation model[29] in combination with the (U)B3LYP hybrid functional and the 6-31G(d) basis set. All calculations were performed using the *Gaussian 09*, rev. D.01.[35]

## Acknowledgements

*Financial support for this project by the Deutsche Forschungsgemeinschaft (SFB 749, Project C6) and the COST action CM1201 is gratefully acknowledged. We furthermore thank Dr. Antonio Herrera for helpful discussions relating to this work.*

## References

[1] a) M. E. Wolff, *Chem. Rev.* **1963**, *63*, 55–64; b) L. Stella, *Angew. Chem.* **1983**, *93*, 368–380; *Angew. Chem. Int. Ed. Engl.* **1983**, *22*, 337–422.
[2] G. Majetich, K. Wheless, *Tetrahedron* **1995**, *51*, 7095–7129.
[3] W. R. Gutekunst, P. S. Baran, *Chem. Soc. Rev.* **2011**, *40*, 1976–1991.
[4] J. L. Jeffrey, R. Sarpong, *Chem. Sci.* **2013**, *4*, 4092–4106.
[5] a) L. R. Reddy, B. V. S. Reddy, E. J. Corey, *Org. Lett.* **2006**, *8*, 2819–2821; b) D. H. R. Barton, A. L. J. Beckwith, A. Goosen, *J. Chem. Soc.* **1965**, 181–190.
[6] P. de Armas, R. Carrau, J. I. Conception, C. G. Francisco, R. Hernandez, E. Suarez, *Tetrahedron Lett.* **1985**, *26*, 2493–2496.
[7] R. Carrau, R. Hernandez, E. Suarez, C. Betancour, *J. Chem. Soc. Perkin Trans. 1* **1987**, 937–943.
[8] R. Hernandez, M. C. Medina, J. A. Salazar, E. Suarez, *Tetrahedron Lett.* **1987**, *28*, 2533–2536.
[9] P. de Armas, C. G. Francisco, R. Hernandez, J. A. Salazar, E. Suarez, *J. Chem. Soc. Perkin Trans. 1* **1988**, 3255–3265.

[10] R. L. Dorta, C. G. Francisco, E. Suarez, *J. Chem. Soc. Chem. Commun.* **1989**, 1168–1169.
[11] A. Yoshimura, V. Z. Zhdankin, *Chem. Rev.* **2016**, *116*, 3328–3435.
[12] K. Muniz, *Top. Cur. Chem.* **2016**, *383*, 105–133.
[13] a) C. Martinez, K. Muniz, *Angew. Chem.* **2015**, *127*, 8405–8409; *Angew. Chem. Int. Ed.* **2015**, *54*, 8287–8291; b) C. Q. O'Broin, P. Fernandez, C. Martinez, K. Muniz, *Org. Lett.* **2016**, *18*, 436–439.
[14] R. Fan, D. Pu, F. Wei, J. Wu, *J. Org. Chem.* **2007**, *72*, 8994–8997.
[15] H. Togo, Y. Hoshina, T. Muraki, H. Nakayama, M. Yokohama, *J. Org. Chem.* **1998**, *63*, 5193–5200.
[16] N. R. Paz, D. Rodriguez-Sosa, H. Valdes, R. Marticorena, D. Melian, M. B. Copano, C. C. Gonzalez, A. J. Herrera, *Org. Lett.* **2015**, *17*, 2370–2373.
[17] M. Katohgi, H. Togo, K. Yamaguchi, M. Yokoyama, *Tetrahedron* **1999**, *55*, 14885–14900.
[18] E. C. Cherney, J. M. Lopchuck, J. C. Green, P. S. Baran, *J. Am. Chem. Soc.* **2014**, *136*, 12592–12595.
[19] Y.-R. Luo, in: *Comprehensive Handbook of Chemical Bond Energies*, CRC Press, London, **2007**.
[20] A. D. Becke, *J. Chem. Phys.* **1993**, *98*, 5648–5652.
[21] a) W. J. Hehre, R. Ditchfield, J. A. Pople, *J. Chem. Phys.* **1972**, *56*, 2257–2261; b) P. C. Hariharan, J. A. Pople, *Theor. Chim. Acta.* **1973**, *28*, 213–222.
[22] D. C. Graham, A. S. Menon, L. Goerigk, S. Grimme, L. Radom, *J. Phys. Chem. A* **2009**, *113*, 9861–9873.
[23] D. J. Henry, M. B. Sullivan, L. Radom, *J. Chem. Phys.* **2003**, *118*, 4849–4860.
[24] A. G. Baboul, L. A. Curtiss, P. C. Redfern, K. Raghavachari, *J. Chem. Phys.* **1999**, *110*, 7650–7657.
[25] J. Hioe, D. Sakic, V. Vrcek, H. Zipse, *Org. Biomol. Chem.* **2015**, *13*, 157–169.
[26] J. Hioe, H. Zipse, *Chem. Eur. J.* **2012**, *18*, 16463–16472.
[27] J. Hioe, H. Zipse, *Encyclopedia of Radical in Chemistry, Biology and Materials*, (Eds.: C. Chatgilialoglu, A. Studer), John Wiley & Sons, New York, **2012**, pp 449–476.
[28] S. J. Blanksby, G. B. Ellison, *Acc. Chem. Res.* **2003**, *36*, 255–263.
[29] A. V. Marenich, C. J. Cramer, D. G. Truhlar, *J. Phys. Chem. B* **2009**, *113*, 6378–6396.
[30] The reaction enthalpy shows very little dependence on the level of theory with by $\Delta H_{298}$(**5a**,G3B3) = −39.8 kJ/mol (G3B3); $\Delta H_{298}$(**5a**,G3(MP2)-RAD) = −39.8 kJ/mol (G3B3); and $\Delta H_{298}$(**5a**,ROB2-PLYP) = −42.2 kJ/mol (G3B3).
[31] Value obtained at G3(MP2)-RAD level. The full systems **9**/**10** were not amenable to full G3B3 calculations.
[32] Q. Qin, S. Yu, *Org. Lett.* **2015**, *17*, 1894–1897.
[33] J. Campos, S. K. Goforth, R. H. Crabtree, T. B. Gunnoe, *RSC Adv.* **2014**, *4*, 47951–47957.
[34] C. Zhu, Y. Liang, X. Hong, H. Sun, W.-Y. Sun, K. N. Houk, Z. Shi, *J. Am. Chem. Soc.* **2015**, *137*, 7564–7567.
[35] *Gaussian 09*, Revision D.01, **2009**. The full citation is available at http://www.gaussian.com/g_tech/g_ur/m_citation.htm.